NORSAR

NORSAR Scientific Report No. 2-2002

Semiannual Technical Summary

1 January - 30 June 2002

Frode Ringdal (ed.)

Kjeller, August 2002

6.3 Design Study for the Refurbishment of the SPITS Array (AS 72)

6.3.1 Introduction

The SPITS array is located on Jansonhaugen in Adventdalen on Spitsbergen, Svalbard, approximately 15 km east-southeast of Longyearbyen. Jansonhaugen is a hill in the middle of a valley (Adventdalen), and the largest part of the array is deployed on the plateau of this hill. The rocks at the site are of Cretaceous age, partly covered by thin top soil or by moraine deposits of variable depth. The twelve sensors of the array are placed at the bottom of nine 6 m deep cased boreholes. The bottom of the boreholes are either in Cretaceous rock or in moraine material in stable permafrost conditions (temperature approximately -5^{o}C all year around at a depth of 6 m), such that there is no melting/freezing taking place at this depth. The 9 array sites are deployed in two rings around a center element (see Fig. 6.3.1). The radii of the rings are approximately 250 m for the A-ring and 500 m for the B-ring. More detailed descriptions of the array and an initial data processing were presented by Mykkeltveit et al. (1992) and Fyen and Ringdal (1993).

As of summer 2002 the SPITS array consists of the following equipment:

- 9 vertical component short-period seismometers, Guralp CMG-3V-borehole, placed at the bottom of 6 m deep cased boreholes.
- 1 three component broad-band seismometer of type Guralp CMG-3T-borehole, also placed at the bottom of the borehole at array site SPB4. This instrument has, however, been out of operation since March 2001.
- 2 Nanometrics RD-6 digitizers, 16-bit resolution, 40 Hz sampling rate.

The transfer function of the SPITS array is shown in Fig. 6.3.2. The yellow dashed circle indicates the highest wavenumber that is likely to be considered for any signals at SPITS, i.e., high frequency Rg-phases (apparent velocity: 1.3 km/s, dominant frequency: 6 Hz). As seen from Fig. 6.3.2, the array exhibits significant sidelobes that are likely to influence the data processing of Rg-phases due to aliasing.

6.3.2 Problematic Signals

We will in this section show some typical examples of signals that are difficult to process properly with the current SPITS configuration. The problems are related to both signal detection, and the estimation of the slowness vector (i.e., apparent velocity and backazimuth) of the detected phases.

The Spitsbergen array (SPITS) often reports a large number of detections (Schweitzer, 1998), which can reach thousands per day. A detailed analysis shows that the majority of these detections are real seismic signals caused by small sources located at close distances. The numerous local events (see e.g., Fig. 6.3.3) typically show P onsets, no well defined S onsets, and dominant Rg onsets. Investigating the mean backazimuths of these Rg phases one can see a strong correlation with the direction to the coal-mine area at about 8 km distance and directions to nearby glaciers (shortest distance about 3 km), for more details see Schweitzer (1998).

At the SPITS array we also observe a relatively large number of high SNR P detections from regional events without any corresponding detection of an S phase. Fig. 6.3.4 shows seismograms observed at the three-component site SPB4 from an earthquake located at the Knipovich

Ridge west of Svalbard at an epicentral distance of about 3°. In addition to the original horizontal components, the rotated radial and transverse components are shown (at the bottom). The S phase has a low SNR and the signal is particularly weak in SV energy, which should be visible on the radial and vertical components. The S phase can, however, be observed on the transverse component SPB4_bt.

Due to the presence of low-velocity materials in the uppermost crust, Sn arrivals from regional events at larger distances also show the largest amplitudes and SNR on the radial or transverse components. As an example, we show in Fig. 6.3.5 SPITS recordings of the Kara Sea event on 16 August 1997. The epicentral distance to this event was 11.6°. The upper trace shows the vertical-component array beam steered with the S-phase apparent velocity of 4.0 km/s. The three lower traces show the vertical, radial and transverse components for the three-component sensor SPB4. All traces of Fig. 6.3.5 are bandpass filtered between 4 and 8 Hz. Notice the improved SNR on the radial and transverse components as compared to the vertical-component S-beam.

6.3.3 Spatial aliasing of high frequency Rg-phases

As seen from Fig. 6.3.2, the transfer function of the SPITS array exhibits significant side lobes that are likely to influence the data processing of the numerous Rg-phases, all having low apparent velocities. The low apparent velocities of the Rg phases are caused by the low seismic velocities of the Cretaceous sediments.

Schweitzer (1998) has introduced a rather complex signal processing scheme to reduce aliasing problems when processing the Rg onsets. There are, however, still cases when Rg phases are mis-identified as P-onsets, and vice versa. In such cases the F-K analysis picks the energy maximum on a sidelobe, in particular for onsets with low SNR.

The numerous local events often contain a mixture of Pg, Sg, and Rg within a time window of 2-5 seconds (see Fig. 6.3.3). In order to estimate the slowness and backazimuth of such onsets, short time windows are needed for the F-K analysis. With the current SPITS configuration we will need at least a 2 s long time window for processing of the low-velocity Rg-phases. For these local events an automatically positioned 2 s long time window often contains all types of phases (Pg, Sg, Rg).

In order to remove the side lobes of the array transfer function and to give us the possibility to analyze the low-velocity onsets in shorter time windows, we propose to install three additional sensors close to the center element SPA0. The geometry of an array cannot be inverted from a given transfer function. It must be found by a trial-and-error search trough different geometries. Therefore, to find a position for the three new sensors, which gives the best suppression of the side lobes in Fig. 6.3.2, we applied a systematic search by adding one station after the other at different locations and calculating the array-transfer function (see e.g., Schweitzer et al., 2002). The searched area was a square of 600*600 m centered at the central site SPA0. In this area all possible site locations on a 5*5 m grid were tested as locations for the new array sensors; the criterion for optimizing the transfer function was to minimize this function in the slowness range between the main lobe and the yellow broken line of Fig. 6.3.2. The best solution found is shown in Fig. 6.3.6 and the location of the three newly proposed sensors SPE1, SPE2, and SPE3 to reach this solution is seen on Fig. 6.3.7. Notice the reduction of the side lobes as compared to Fig. 6.3.2.

6.3.4 Low resolution of the F-K estimates

As seen from Fig. 6.3.6, the transfer function of the SPITS array, including the three new sites in the center, has a relatively wide main lobe. This feature limits the resolution capability of the array, which is critical for classifying signals as local, regional or teleseismic based on the apparent velocity estimates from the F-K analysis. In addition, the backazimuth estimates from the F-K analysis have large uncertainties.

In order to narrow the main lobe we have to extend the aperture of the array. Based on experience with other regional arrays in Fennoscandia (FINES, ARCES and NORES) we propose to install new instruments in a C-ring like configuration. The plateau on the hill on which SPITS is located is surrounded by steep slopes and rivers both to the north and south, and the array can therefore not be extended in these directions. From analysis of topography maps, satellite photos, and from inspections during visits to the SPITS array we propose a new configuration as shown in Fig. 6.3.7: three C-ring sites towards east (SPC1, SPC2, SPC3) and three C-ring sites towards west-southwest (SPC4, SPC5, SPC6). The exact positions of these additional six new C-ring sites were also found by a systematic trial-and-error search on a 10*10 m grid. The array-transfer function, for which the main lobe became the smallest, was chosen as the best one.

The transfer function of the new configuration of the SPITS array, i.e. the original nine sites extended by three sites in the center (SPE1, SPE2, SPE3) and six sites in the C-ring (SPC1, SPC2, SPC3,SPC4, SPC5, SPC6) is shown in Fig. 6.3.8. Notice that the main lobe has become narrower as compared to Figs. 6.6 and 6.2, and that it is elongated in the north-south direction due to the non-circular array geometry. The relative coordinates of all sites with respect to the center site SPA0 are listed in 6.4.1.

6.3.5 Detection and F-K analysis of S-phases

As shown in Figs. 6.4 and 6.5, regional S-phases at SPITS in general have the largest amplitudes and SNR on the horizontal components. The current SPITS configuration has only one three-component instrument at site SPB4. This instrument has, however, been quite unstable in operation. In order to detect S-phases more efficiently, more three component instruments are needed. While one three-component instrument already improves the detection capability of S-phases (see Figs. 6.4 and 6.5), the subsequent F-K analysis would suffer from low SNR as the vertical component sensors have to be used for this purpose.

With more three-component sites, the detection capability of S-phases can be further improved by creating S-velocity beams from the rotated radial and transverse components, as now done for ARCES and NORES (Kværna et al., 1999). In addition, the F-K analysis can now be run on the horizontal components, as e.g., demonstrated by Schweitzer (1994).

As a first attempt, we calculate the array response of 4 three-component sensors, which is a minimum number of traces for running an F-K analysis. After testing several combinations of the SPITS geometry, our best result was obtained by using SPA1, SPC3, SPC4 and the already existing three-component sensor SPB4 (see Fig. 6.3.7). With only four sensors we were unable to remove all side lobes from the S-phase wavenumber range, but we can obtain a relatively narrow main lobe. However, with four sensors only, we will lose the capability to run an F-K analysis on the horizontal components in the case that one of the horizontal sensors is down. The best “realistic” three-component configuration was obtained by having three-component

instruments at all five B-ring sites and at SPA0 in the center. Such a configuration can improve the SNR for S onsets by a factor of about 2.5; the corresponding transfer function of Fig. 6.3.9 shows no side lobes within the wavenumber range for regional Sn phases (i.e., between the red and the yellow rings).

6.3.6 Sampling rate, high-frequency spectra, and 24 bits digitizers

With the current sampling rate of 40 Hz at SPITS, we can conduct array processing for signal frequencies up to 16-20 Hz. For higher frequencies the coherency among the signals at the different sensors is heavily reduced such that beamforming and F-K analysis have little effect. Therefore, we see no need to increase the general sampling rate for SPITS.

However, it is well known that we at SPITS observe high signal frequencies (e.g., Bowers et al., 2001). Therefore we suggest that one of the three-component sensors (e.g., SPA0) is sampled at 120 Hz, or alternatively 80 Hz.

In order to meet the standard of the CTBT International Monitoring System an upgrade of the digitizers to 24 bit words is needed.

6.3.7 Conclusion

In conclusion, the following extensions are suggested for the SPITS array to increase its detection and monitoring capabilities:

- Three new sites in the center of the array (SPE1, SPE2, SPE3) equipped with vertical component instruments.
- Six new sites in a C-ring equipped with vertical component instruments.
- Add 5 three-component instruments to SPA1, SPB1, SPB2, SPB3 and SPB5. The existing broad-band three-component instrument at SPB4 can be used for array processing after digitally reshaping the response.
- Install 24 bits digitizer for all channels.
- Sample one of the three-component sensors at 120 Hz, e.g., SPA0.

Johannes Schweitzer
Tormod Kværna

References

Bowers, D., P. D. Marshall and A. Douglas (2001): The level of deterrence provided by data from the SPITS seismometer array to possible violations of the Comprehensive Test Ban in the Novaya Zemlya region. *Geophys. J. Int*., 146, 425-438.

Fyen, J and F. Ringdal (1993): Initial processing results for the Spitsbergen small-aperture array. Semiannual Technical Summary, 1 October 1992 - 31 March 1993, NORSAR Scientific Report 2-92/93, 119-131.

Kværna, T., J. Schweitzer, L. Taylor and F. Ringdal (1999): Monitoring of the European Arctic Using Regional Generalized Beamforming. Semiannual Technical Summary, 1 October 1998 - 31 March 1999, NORSAR Scientific Report 2-98/99, 78-94.

Mykkeltveit, S., A. Dahle, J. Fyen, T. Kværna, P.W. Larsen, R. Paulsen, F. Ringdal and I. Kuzmin (1992): Extensions of the northern Europe regional array network -- new small-aperture arrays at Apatity, Russia, and on the Arctic Island of Spitsbergen. Semiannual Technical Summary, 1 April - 30 September 1992, NORSAR Scientific Report 1-92/93, 58-71.

Schweitzer J. (1994): Some improvements of the detector / SigPro-system at NORSAR. Semiannual Technical Summary, 1 October 1993 - 31 March 1994, NORSAR Scientific Report 2-93/94, 128-139.

Schweitzer J. (1998): Tuning the automatic data processing for the Spitsbergen array (SPITS). Semiannual Technical Summary, 1 April - 30 September 1998, NORSAR Scientific Report 1-98/99, 110-125.

Schweitzer, J., J. Fyen, S. Mykkeltveit and T. Kværna (2002): Seismic Arrays. **In**: P. Bormann (ed.), 2002: *New Manual of Seismological Observatory Practice*, Chapter 9, 52 pp. (in press).

Table 6.3.1. The relative coordinates of the old and newly proposed sites of the SPITS array with respect to the central element SPA0, which is located at 78.1777° N and 16.36998° E.

Site	X (E-W) [m]	Y (N-S) [m]
SPA0	0	0
SPA1	125	227
SPA2	150	-202
SPA3	-255	-44
SPB1	470	228
SPB2	333	-381
SPB3	-255	-451
SPB4	-501	123
SPB5	-49	513
SPE1	150	-30
SPE2	-30	-160
SPE3	-230	-240
SPC1	1030	500
SPC2	1100	-200
SPC3	745	-240
SPC4	-800	-835
SPC5	-710	-460
SPC6	-1140	-40

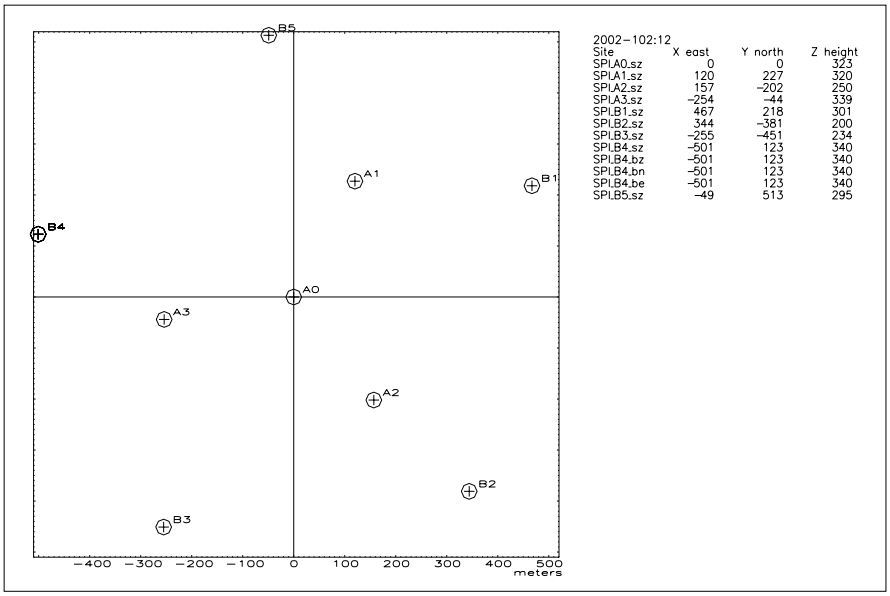

Fig. 6.3.1. *Current geometry of the SPITS array.*

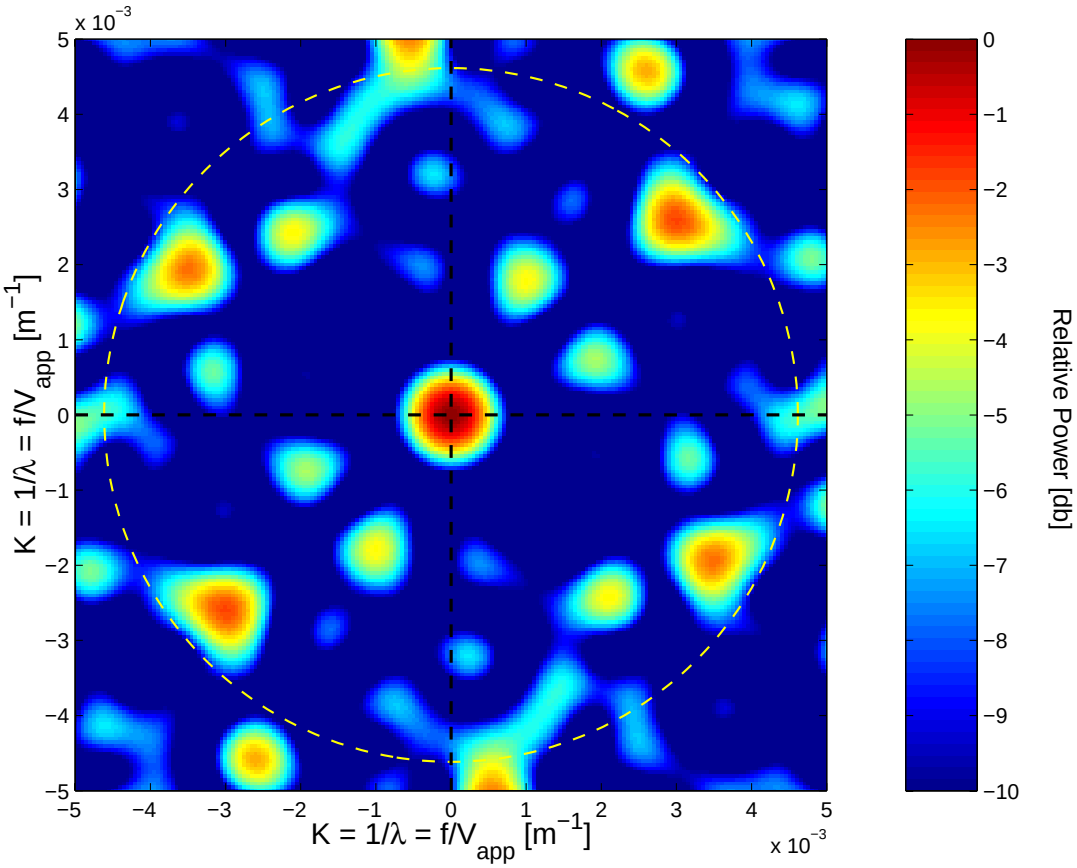

Fig. 6.3.2. *The transfer function of the current SPITS array (vertical components).*

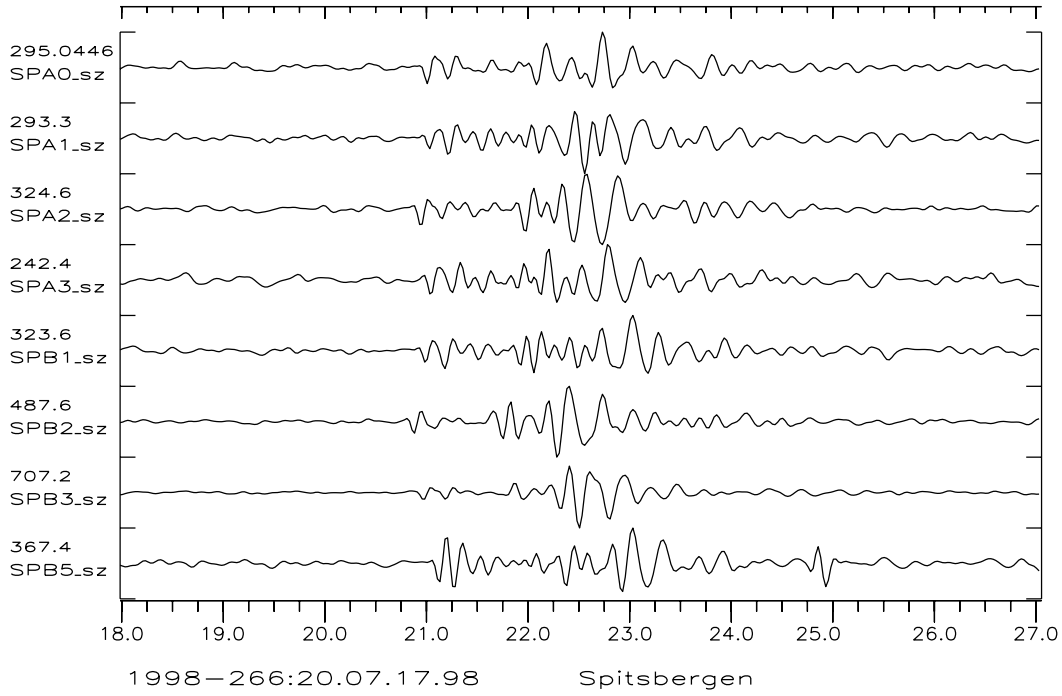

Fig. 6.3.3. *Example of a local event observed at SPITS, located in the glacier Gløttfjellbreen (backazimuth = 141°, D = 4 km). The traces are the band pass filtered (3-8 Hz) vertical-component seismograms.*

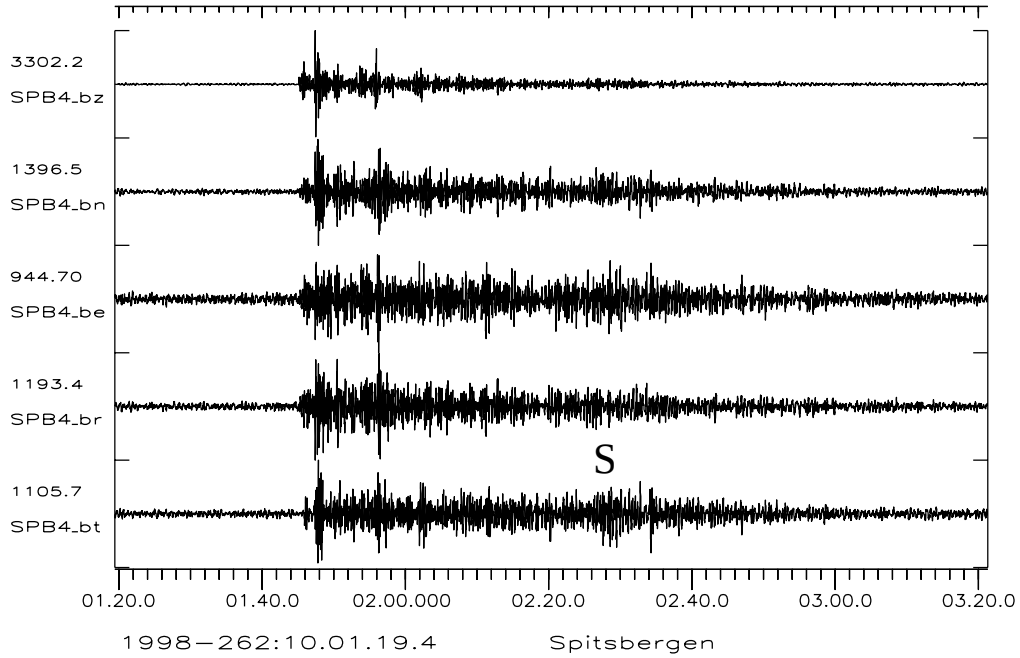

Fig. 6.3.4. *Filtered seismograms (3-6 Hz) at the three-component site SPB4 from an earthquake located at the Knipovich Ridge northwest of Svalbard at an epicentral distance of about 3°. The rotated radial and transverse components are shown (at the bottom).*

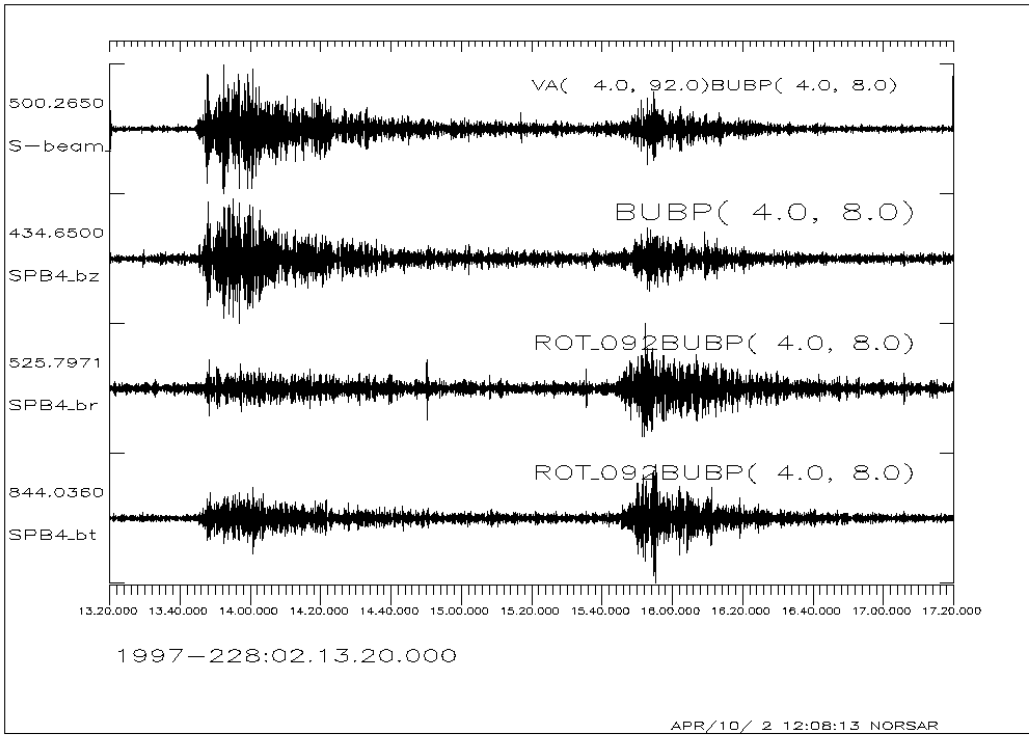

Fig. 6.3.5. *SPITS observations of the Kara Sea event on 16. August 1997. The upper trace shows the vertical-component array beam steered with the S-phase apparent velocity of 4.0 km/s. The three lower traces show the vertical, radial and transverse components for the three-component sensor SPB4. All traces are bandpass filtered between 4 and 8 Hz.*

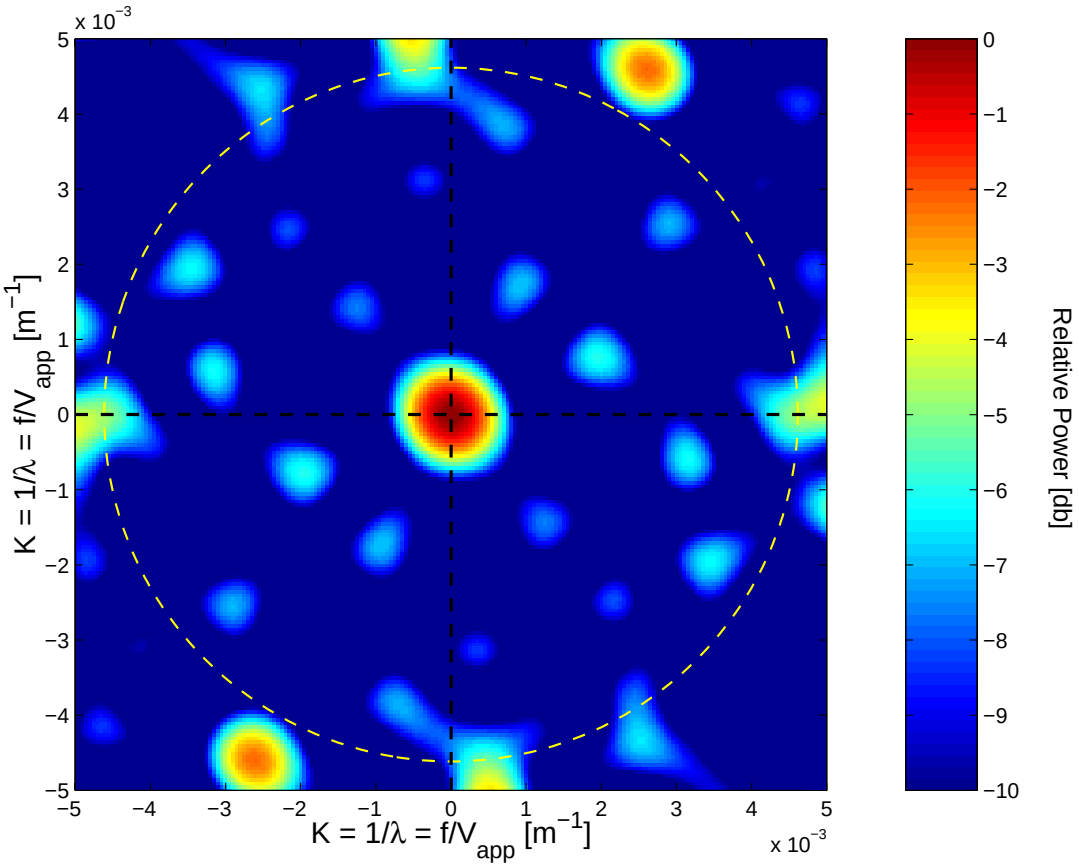

Fig. 6.3.6. *The transfer function of the SPITS array extended by three sites (SPE1, SPE2, SPE3) in the center, note the side-lobe reduction inside the yellow ring with respect to Fig. 6.3.2.*

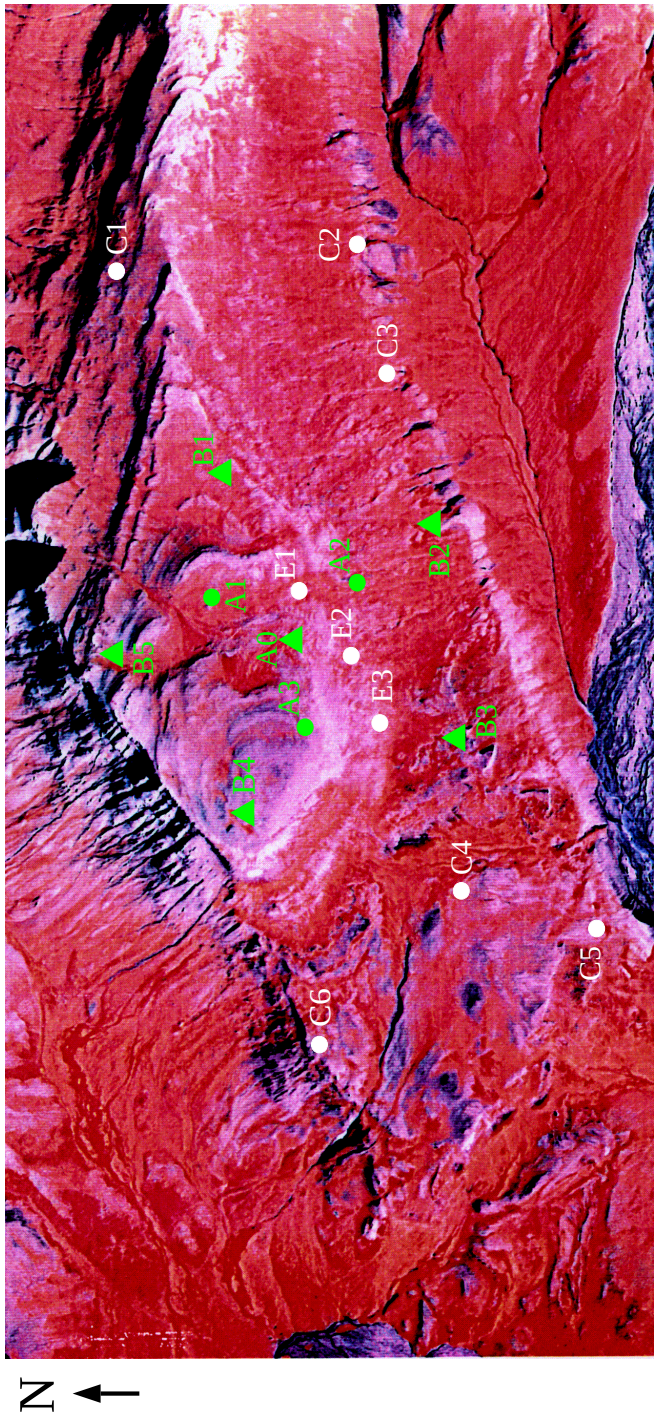

Fig. 6.3.7. *The suggested extended configuration of the SPITS array plotted on a satellite photo of Jansonhaugen. The original configuration is extended by three sites (E1, E2, E3) in the center and six sites in the C-ring (C1, C2, C3, C4, C5, C6). Green symbols: sites unchanged from the old configuration. White circles: new sites equipped with vertical component sensors. Green triangles: Sites of the old configuration upgraded to three-component sensors. High-frequency sensor: the three-component instrument at A0 should be sampled at e.g., 120 Hz.*

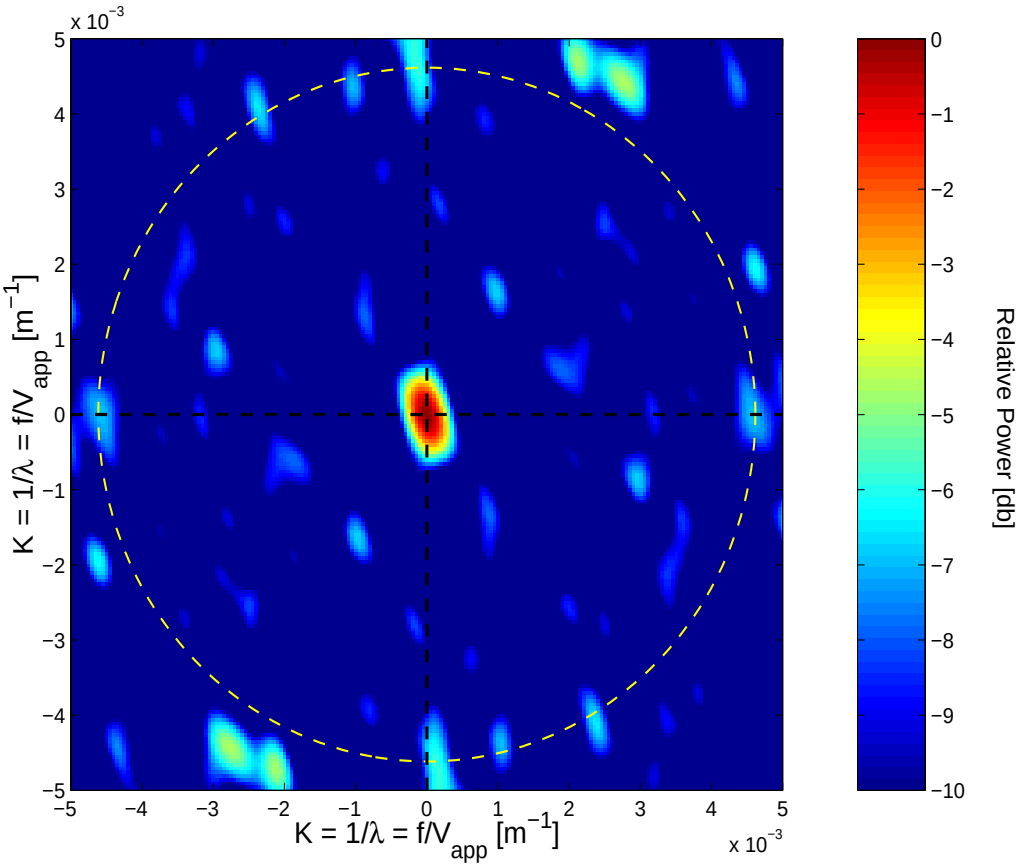

Fig. 6.3.8. *The transfer function of the new SPITS array configuration for vertical sensors at all sites as shown on satellite picture in Fig. 6.3.7.*

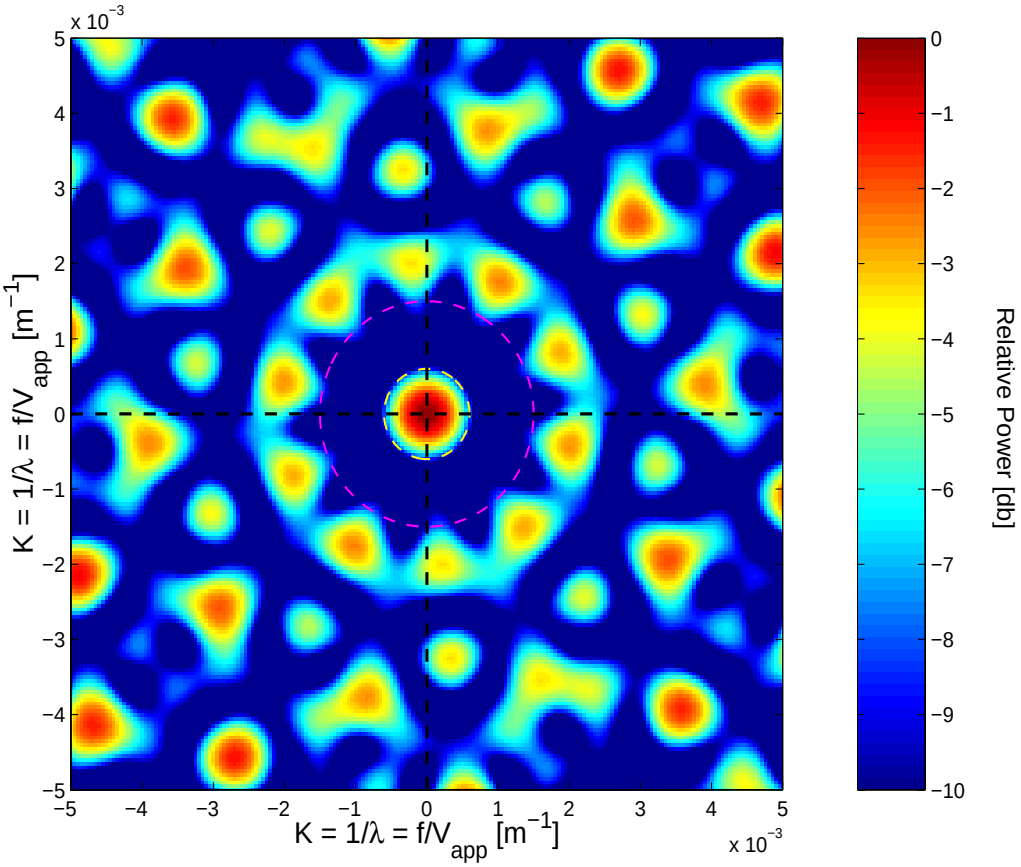

Fig. 6.3.9. *The transfer function of the 6 SPITS array sites SPA0, SPB1, SPB2, SPB3, SPB4 and SPB5. The yellow and red circles represent the wavenumber range for regional Sn phases.*